

Feature Extraction Based on ORB- AKAZE for Echocardiogram View Classification

Original Scientific Paper

1. Shamla Beevi A.

Department of Computer Science and Engineering
National Institute of Technology Calicut,
Kerala, India
beeishamla471@gmail.com

2. Ratheesha S.

SOTI India Private Limited,
Kochi, Kerala, India

3. Saidalavi Kalady

Department of Computer Science and Engineering
National Institute of Technology Calicut,
Kozhikode, Kerala, India

4. Jenu James Chakola

Department of Cardiology
Aster MIMS Hospital Kottakkal
Malappuram Kerala, India

Abstract – In computer vision, the extraction of robust features from images to construct models that automate image recognition and classification tasks is a prominent field of research. Handcrafted feature extraction and representation techniques become critical when dealing with limited hardware resource settings, low-quality images, and larger datasets. We propose two state-of-the-art handcrafted feature extraction techniques, Oriented FAST and Rotated BRIEF (ORB) and Accelerated KAZE (AKAZE), in combination with Bag of Visual Word (BOVW), to classify standard echocardiogram views using Machine learning (ML) algorithms. These novel approaches, ORB and AKAZE, which are rotation, scale, illumination, and noise invariant methods, outperform traditional methods. The despeckling algorithm Speckle Reduction Anisotropic Diffusion (SRAD), which is based on the Partial Differential Equation (PDE), was applied to echocardiogram images before feature extraction. Support Vector Machine (SVM), decision tree, and random forest algorithms correctly classified the feature vectors obtained from the ORB with accuracy rates of 96.5%, 76%, and 97.7%, respectively. Additionally, AKAZE's SVM, decision tree, and random forest algorithms outperformed state-of-the-art techniques with accuracy rates of 97.7%, 90%, and 99%, respectively.

Keywords: Ultrasound, Echocardiography, SRAD, ORB, AKAZE

1. INTRODUCTION

1. INTRODUCTION

Cardiac echocardiography produces images that assist experts in determining the function and diseases related to the human heart. Unlike magnetic resonance imaging (MRI), X-Ray, and computed tomography (CT) scans, ultrasound (US) imaging is free from radiation and is highly portable [1]. Echocardiography is an ultrasound medical imaging modality for obtaining cross-sectional views of the human heart. They support doctors in the visualization of valve failure, blood clots, changes in the velocity of blood inflow and outflow, chamber enlargement, damaged tissues, and muscles [2,3]. Doctors frequently recommend a 2D transthoracic echocardiogram (TTE), in which high-frequency US waves from a probe or transducer are placed over standard locations on the anterior chest wall to obtain different heart views. Different anatomical sections or views are obtained by adjusting or tilting the plane of waves that pass through the body. Standard views include parasternal long-axis (PLAX) view, parasternal short-axis (PSAX) views, apical

2-chamber (A2C) view, apical 4-chamber (A4C) view, apical 5-chamber (A5C) view, subcostal view, the suprasternal view that provide clear anatomy of heart [4-6]. A transesophageal echocardiogram inserts a tube through the oesophagus to create a close-up view of the heart. Complicated cases, including infants and children, are studied and analyzed with 3D echocardiography to create detailed 3D images before surgeries [7]. Echocardiography is an essential diagnostic tool in cardiology. Cardiac-related diseases like cardiomyopathies, ventricular dysfunction, coronary artery disease (CAD), congenital diseases, left ventricular hypertrophy (LVH), pulmonary hypertension, and stenosis is identified by skilled sonographers and experts by analysis of echocardiogram(echo) images [1]. However, the need for skilled experts in the interpretation of echo images has hindered the public from obtaining comprehensive benefits. We use the potentials of image processing and computer vision to address these shortcomings in echocardiogram analysis.

Deriving information from images automates various decision-making processes in medicine, industry, auto-

mobiles, surveillance, defense, and many more fields. In recent years, handcrafted features extracted from data and fed into Machine learning (ML) models have outperformed human abilities in similar tasks. Sophisticated advancements, including feature extraction and representation with deep networks, have exponentially increased the capabilities of computer vision for building novel solutions in various fields. Application of computer vision in echocardiogram images for automated view identification and disease diagnosis can considerably impact rural areas that lack human expertise and other resources. Ultrasound images are corrupted with speckle noise, which shows multiplicative and granular behavior [8]. Speckle removal in echocardiogram medical images helps easily interpret the diseased tissue [9]. Extracting relevant features such as local patches, textures, color information, and edges from medical images and categorizing these images using a machine learning model continues to bring a massive leap in health care. In this paper, we propose an automated view classification model for echocardiogram images based on feature vectors obtained from Oriented Fast and Rotated Brief (ORB) and Accelerated KAZE (AKAZE), followed by the feature representation approach bag of visual words (BOVW). Four primary views of echo images were classified using machine learning classifiers such as support vector machine (SVM), decision tree, and random Forest classifier, and their performance was assessed.

The primary contributions of this work are:

- A pipeline for classifying echocardiographic images using machine learning techniques has been developed.
- Speckle was removed from echocardiographic images using the SRAD method to improve classification accuracy.
- ORB and AKAZE were used to perform cost-effective manual feature extraction from echocardiographic images, and features represented using the BoVW method.
- Our results demonstrated superior results compared to various machine learning models for classifying echo images.

The structure of this paper is as follows: The related work in handcrafted feature extraction, feature representation, and ML models for medical image classification is discussed in section 2, along with despeckling of ultrasound images. The materials and techniques used for our study are the focus of section 3. Section 4 contains the results, and Section 5 contains the conclusion and an explanation of the future direction of our work.

2. RELATED WORKS

This study focused on the noise reduction and feature extraction of echocardiographic images. We first extracted features using the AKAZE and ORB methods,

and then classified the data using different machine-learning models. This section discusses previously written literature on the previously stated modules.

2.1. DESPECKLING OF ULTRASOUND MEDICAL IMAGES

Benzarti et al. proposed an integrated method for denoising medical images using logarithmic transformation and a nonlinear diffusion tensor [9]. Speckle noise is multiplicative, and logarithmic transformation converts multiplicative noise to additive [10]. performed a comparative study on spatial and frequency domain denoising filters on ultrasonic B-mode images. They quantitatively analyzed the performance of the filters in terms of Peak Signal Noise Ratio (PSNR) value. Durte-Salazar et al. [8] explained 27 different methods that eliminate speckle noise in medical ultrasound images, which extensively covers conventional methods like spatial, diffusion, wavelet filtering, and recent techniques based on deep learning [11]. Evaluated the performance of different filtering methods like frost, mean, Kuan, median, and speckle-reducing anisotropic diffusion filter (SRAD) on liver US image data. SRAD filter showed better results on denoising medical ultrasound images from their experiments.

2.2. FEATURE EXTRACTION TECHNIQUES

It is possible to reduce image dimensions and, as a result, processing costs by selecting significant features that highlight the images' inherent content. Tareen et al. presented a comparative study on the performance of various feature extraction algorithms, SIFT, SURF, KAZE, AKAZE, ORB, and BRISK, that can be extensively applied for image registration [12]. Quantitative comparisons between these methods were mainly made based on several key points and corners, feature descriptors identified, and computational cost. Wei Li et al. proposed AKAZE for extracting salient features from echocardiogram videos and compared the performance with SIFT extraction technique [13]. Feature representation methods like a bag of words (BOW), sparse coding, and fisher vector (FV) are utilized to classify eight viewpoints. ORB feature matching was suggested by Rublee et al. for significant applications, including object recognition and patch-tracking on a smartphone [14]. Their study confirmed that ORB is a substitute to SIFT or SURF. Chhabra et al. developed content-based image retrieval (CBIR) system with the descriptors obtained from SIFT and ORB [15]. K-means clustering is applied to descriptors of every image to form 32 clusters, and the mean of these clusters constitutes the 32D feature vector. They also utilized locality-preserving projection (LPP) for dimensionality reduction [16]. Examined traditional approaches for extracting remarkable object recognition features such as Bag of Words, HOG-SVM (Histogram of Oriented Gradients-Support Vector Machine), and deep learning-based methods CNN and pre-trained Alexnet CNN.

2.3. FEATURE REPRESENTATION TECHNIQUES

Representing extracted features from images that are representative and discriminative is essential to develop classification models [17]. Presented an optimal correlation-based BOVW model and utilized the modest visual dictionary to implement image classification. Caeleu et al. presented a bag of features (BoF) approach to develop a histogram of visual words for binary classification of liver lesions in the CEUS dataset [18]. Tiang et al. conducted a comprehensive survey on the latest image feature extraction and representation techniques focusing on the fusion of global and local features for CBIR and automatic image annotation [19]. They also looked into generating visual-word image representations using vector-quantized region features [20]. Proposed a feature representation for microscopy image classification. A feature representation for microscopy image classification was proposed by [20]. They created feature vector (FV) descriptors from different local features and a separation-guided dimension reduction (SDR) model to transform the FV descriptors to low dimensionality [21]. Developed a sparse coding-based key point detector for low-dimension mapping of descriptors retaining complete discriminative features.

2.4. MACHINE LEARNING FOR MEDICAL IMAGE CLASSIFICATION

Image classification requires subtle features to be extracted from each image so that discriminating attributes can make efficient categorization or recognition. K. S. Jothi et al. [17] proposed a heart disease prediction model based on the Decision Tree and k-nearest neighbor (KNN) algorithms, two popular data mining algorithms, and obtained promising results in terms of accuracy. Presented eight machine learning algorithms for classifying major stroke types, ischemic and hemorrhage. u Random forest classifier performed better

than other algorithms with an accuracy of 95.97%. Introduced a random forest algorithm with a correlation-based feature selection approach for early diagnosis of heart disease on the UCI heart database. Designed a classification model combining particle swarm optimization (PSO) and SVM for brain tumour prediction. Intensity, shapes, and texture-based features were derived from segmented MRI images to build a subset of relevant features. Thepage and Jadhav [19] investigated on covid-19 chest X-Ray database for automatic identification of virus infection. The feature set obtained via local binary patterns (LBP) was used to a train random tree - random forest - KNN ensemble model, which showed convincing results.

3. MATERIALS AND METHODS

This section describes the dataset, tools and libraries, and methods used in this study.

3.1. DATASETS

The dataset for this study was obtained from Aster MIMS Hospital Kottakkal in Kerala, India, with the approval of the Scientific Research Committee (SRC) and the institutional ethics committee (IEC). The dataset includes 112 echocardiogram videos collected from 56 patients (including 31 regional wall motion abnormalities and 25 normal cases). Each frame obtained is of size 600 x 800 pixels. All images were acquired using the Philips Epiq 7C cardiology US system. Echocardiogram videos are stored in digital imaging and communications in medicine (DICOM) format and sampled at a rate of 15 frames per second. Cropping was used to remove from each image information related to image acquisition, identifying information, and other information outside the image sector. These images were resized to 200 X 200 pixels. Figure 1 shows sample images from the dataset.

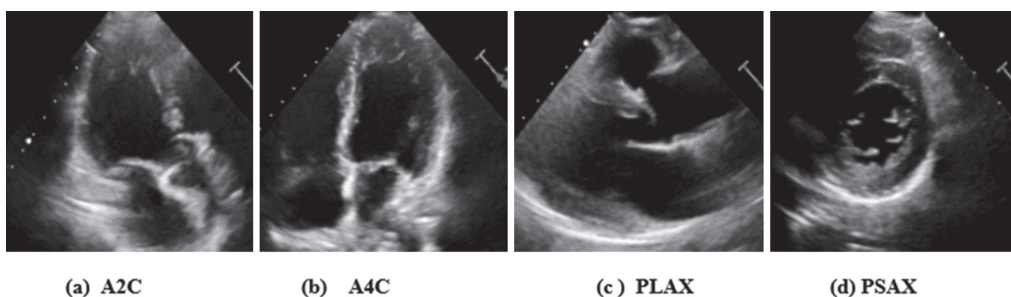


Fig. 1. Four views of echocardiogram image (a)A2C (b)A4C (c)PLAX (d)PSAX

The four categories of views are present in the dataset, namely: A2C, A4C, PLAX, and PSAX. Table 1 shows the distribution of data by views. Table 1. Distribution of data in the collected dataset.

Table 1. Distribution of data in the collected dataset

View	A2C	A4C	PLAX	PSAX	Total
Images	401	401	404	401	1604

3.2. LIBRARIES AND TOOLS

We employed the Python programming language and the Spyder integrated development environment (IDE) for our experiment. Several Python libraries were used to create the models, including numpy, pandas, matplotlib, sklearn, seaborn, and scipy. Additionally, we prepared the dataset, edited images, produced visual representations, and plotted the outcomes in Spyder.

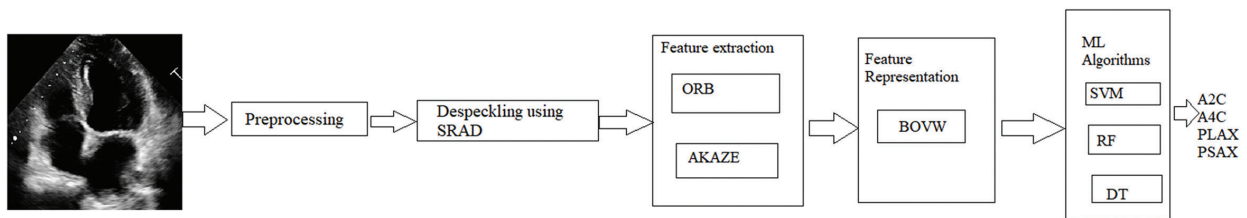


Fig. 2. Architecture of the proposed system

Figure 2 shows the pipeline architecture of our proposed system. It includes mainly four modules: Denoising echo images using speckle reducing anisotropic diffusion filter (SRAD) method, feature extraction using ORB (Oriented FAST and Rotated BRIEF) and AKAZE(Accelerated-KAZE), feature representation using a bag of words (BoW) and classification using different machine learning algorithms SVM, Decision tree and random forest classifier.

3.3. DESPECKLING USING SRAD

This study used the SRAD method to remove speckle noise from the echo image. It is a partial differentiation technique proposed by Yu and Acton in 2002 [10] to reduce speckle noise in ultrasound images. It is a useful method for maintaining edge and detail while lowering noise. The square speckle scale function is computed using this method by considering the image's mean and variance. The diffusion coefficient is calculated using the normalized discrete Laplacian and the

normalized discrete gradient magnitude, as well as the gradient direction. It is presented in equation (3). Equation (4) provides the formula for the instantaneous coefficient of variation (ICOV) (4). Equation (1) and (2) contains the expression for partial derivatives.

$$\frac{\partial I(x,y,t)}{\partial t} = \text{div}[c(q)\nabla I(x,y,t)] \quad (1)$$

$$I(x,y,t) = I_0(x,y,t) \frac{\partial I(x,y,t)}{\partial n} \Big|_{\partial \Omega} \quad (2)$$

$c(q)$: coefficient of diffusion; ∇ : gradient operator; div : divergence operator; $I_0(p,q)$: image intensity.

$$c(q) = \frac{1}{1 + \frac{[q^2(x,y) - q_0^2(t)]}{[q_0^2(t) - q_0^2(9t)]}} \quad (3)$$

$q(x,y,t)$: instantaneous variation coefficient

$$q = \frac{\sqrt{\frac{1}{2}(\nabla I)^2 - \left(\frac{1}{4}\right)^2 \left(\frac{\nabla^2 I}{I}\right)^2}}{\left[1 + \left(\frac{1}{4}\right)\left(\frac{\nabla^2 I}{I}\right)^2\right]} \quad (4)$$

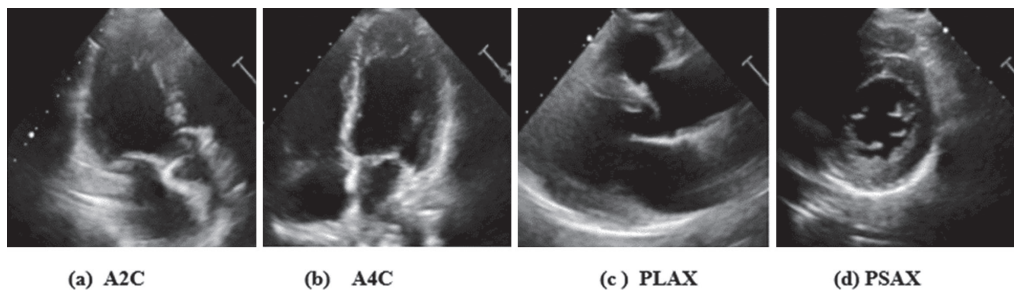


Fig. 3. Denoised Images using SRAD (a)A2C (b)A4C (c)PLAX (d)PSAX

Figure 3 shows the denoised echo images after applying the SRAD method. Denoised images will help to improve the accuracy of image view classification.

3.4. FEATURE EXTRACTION USING ORB AND A-KAZE

Scale-invariant feature transform (SIFT), speeded-up robust features (SURF), features from accelerated segment test (FAST), binary robust independent elementary features (BRIEF), ORB, KAZE, and AKAZE are key point-based 2D feature detection algorithms. ORB was proposed [11]. This sophisticated method combines the BRIEF descriptor and the FAST keypoint detector and replaces SIFT and SURF, a scale and rotation invariant feature extraction method. The magnitude is

ten times and 100 times faster when comparing ORB to SURF and SIFT. [12-13]. KAZE is a nonlinear diffusion filtering method based on partial differential equations (PDEs). AKAZE reduces the feature extraction complexity by fast explicit diffusion (FED). Compared to KAZE and AKAZE, the main drawback of other feature extraction techniques is their high computational expense. In our experiments, we used the ORB method to extract 500 key points, each of which had a 32-element descriptor, from the denoised echo image, and the AKAZE method discovered roughly 450 key points, each of which had a 61-element descriptor. View prediction requires extracting features that distinguish between the different echocardiogram views.

The main disadvantage of hand engineering techniques is that they are highly data-dependent.

Feature extraction plays a critical role in building superior machine learning models by avoiding the inconvenience of training and developing extensive

data-driven deep networks in low-resource settings. Accurate representation of features is critical for producing accurate results.

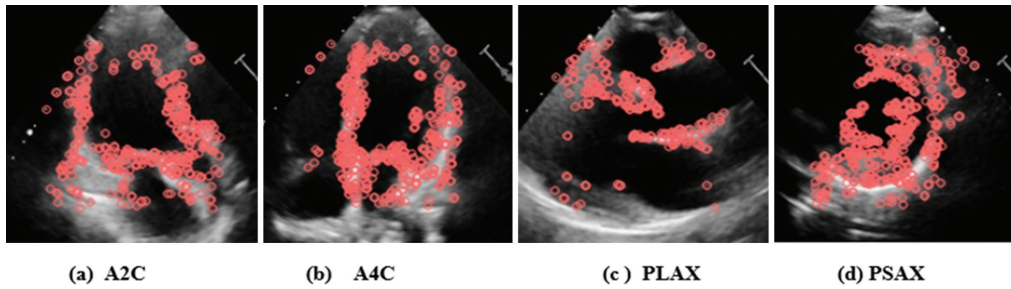
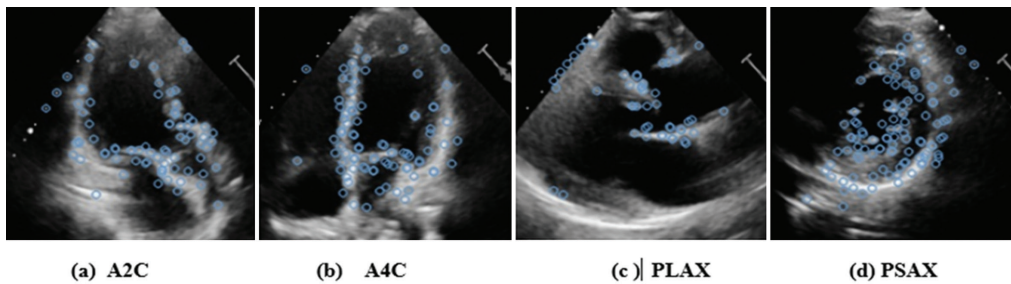


Fig. 4. Key points extracted by ORB (a)A2C (b)A4C (c)PLAX (d)PSAX



Figures 4 and 5 show features extracted using the ORB and AKAZE methods, respectively. Even though the ORB method can extract more features than the AKAZE method, the latter can extract more relevant features.

3.5. FEATURE REPRESENTATION USING BOVW

BOVW, the feature representation concept used in computer vision, is borrowed from the bag of words

(BOW) method in natural language processing (NLP) [14-16]. Keypoints and descriptors used to construct a visual dictionary after clustering and frequency histogram of features define each image's feature vector. Code words in the vocabulary are the most relevant features, and the histogram shows the count of occurrence of these features in the entire image set. Figure 6 shows the histogram of a bag of visual words using ORB and AKAZE feature extraction techniques.

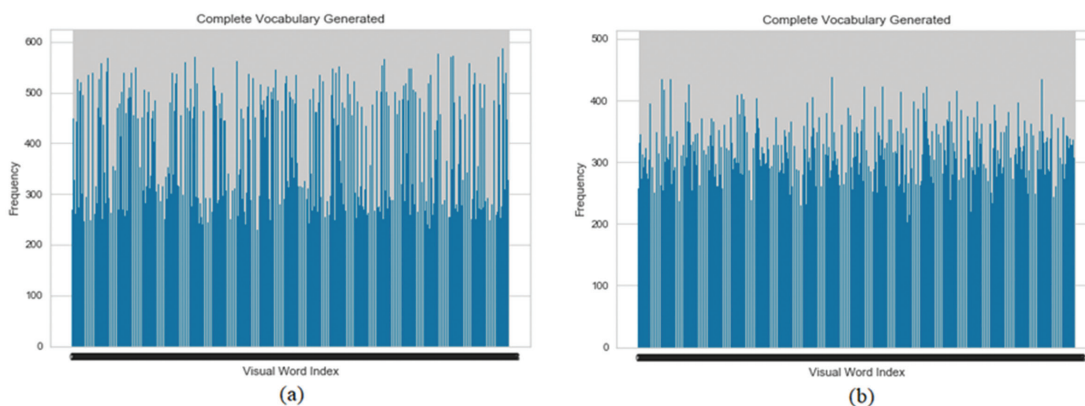


Fig. 6. Histogram of Visual words obtained from (a) ORB and (b) AKAZE

3.6. ECHOCARDIOGRAM VIEW CLASSIFICATION USING ML MODELS

Fig. 1 depicts the proposed system's architecture. Initially, the input image is preprocessed, and then the SRAD algorithm is used to eliminate speckle noise. The input image is first preprocessed, and then the SRAD algorithm is used to remove speckle noise. ORB and AKAZE were used

to extract features from these denoised images. Key point descriptors from ORB and AKAZE were clustered into 1024 visual words using the k-means algorithm. We fed the feature vectors generated by ORB and AKAZE to three different ML algorithms for the classification of 4 primary echocardiogram views. Supervised models SVM, decision tree, and random forest classifier [17-20] trained using feature vectors labelled with corresponding views.

Table 2. Performance comparison between ML models

Feature extraction Method	ML Model	Accuracy (%)	Specificity (%)	Sensitivity (%)	Precision (%)
ORB	SVM	96.5	96.57	97	97
ORB	Decision Tree	76	75.5	76	76
ORB	Random Forest	97.7	97.7	95	98
AKAZE	SVM	97.7	97.7	98	98
AKAZE	Decision Tree	90	89.9	90	90
AKAZE	Random Forest	99	99	99	99

Four standard views labeled on the images are A2C, A4C, PLAX, and PSAX. The models were trained over 1205 images and tested with 402 images. For both feature extraction techniques, confusion matrix and classification reports were found for each model to compare their performance.

3.7. PERFORMANCE MEASURES

Various performance assessment metrics have been applied to the performance evaluation of the classifiers. Mathematical expressions for accuracy, specificity, sensitivity, and precision are shown in equations (5), (6), (7), and (8). - These metrics can be calculated from the confusion matrix. The confusion matrix assists practitioners in determining whether the results are of high performance.

The model's accuracy refers to the total number of correct predictions over a total number of predictions. It is given by equation (5).

$$\text{Accuracy} = \frac{T_P + T_N}{T_P + T_N + F_P + F_N} \tag{5}$$

Specificity indicates the proportion of actual false samples, which the model predicted as a false sample itself. The formula for specificity is given in equation (6).

$$\text{Specificity} = \frac{T_N}{T_N + F_P} \tag{6}$$

Sensitivity or recall tells the ratio of samples predicted true over the actual true samples. It is given by equation (7).

$$\text{Sensitivity} = \frac{T_P}{T_P + F_N} \tag{7}$$

Precision is a metric that calculates the proportion of true positives to the sum of true positives and false positives. Equation (8) provides it.

$$\text{Precision} = \frac{T_P}{T_P + F_P} \tag{8}$$

The area under the curve (AUC) of the Receiver operator characteristic (ROC) curve is a graphical representation of the performance of our machine learning classifier. The higher the AUC, the better the model performance. It depicts the trade-off between false positive rates plotted along the X-axis and true positive rates along the Y-axis.

4. RESULTS

Figures 1, 3, 4, and 5 display the four main views of an echocardiogram, denoised image using SRAD, key points detected using ORB, and key points detected using AKAZE, respectively.

Performance comparisons in terms of accuracy, specificity, sensitivity, and precision among ML models used for the experiment based on ORB and AKAZE have been presented in Table 2. AKAZE and ORB coupled with Random Forest showed excellent performance with an overall accuracy of 99 % and 97.7%.

The ROC curve for the view classification of three ML models with ORB and AKAZE feature extraction methods used for the study can see in figs 7 and 8. The ROC curve offers a graphic representation of a classifier's effectiveness. The area under the ROC curve, or AUC, provides a scalar metric that sums up the classifier's effectiveness. An improved classifier will have a higher AUC value, with 1 denoting the ideal classifier. The normalized confusion matrix exhibiting the performance of the Random Forest classifier with AKAZE is depicted in Figure 9. From the confusion matrix, we can demonstrate that our findings are sound.

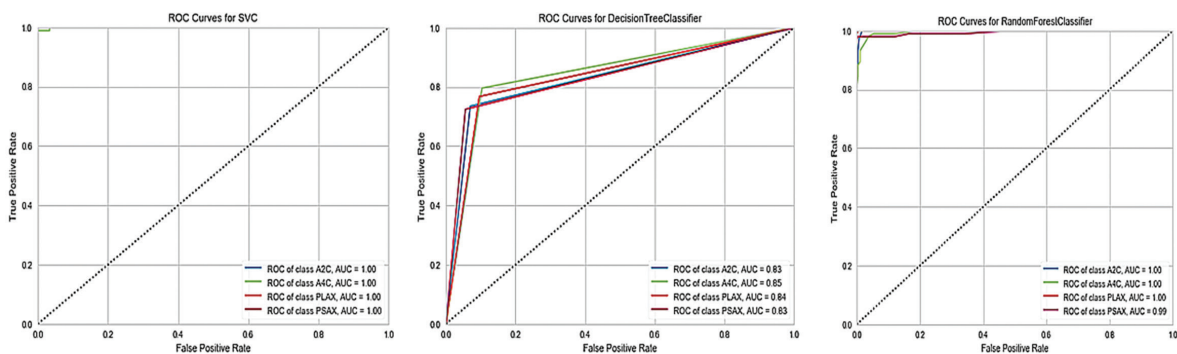


Fig. 7. ROC curve of ORB with SVM, Decision Tree and Random Forest classifier

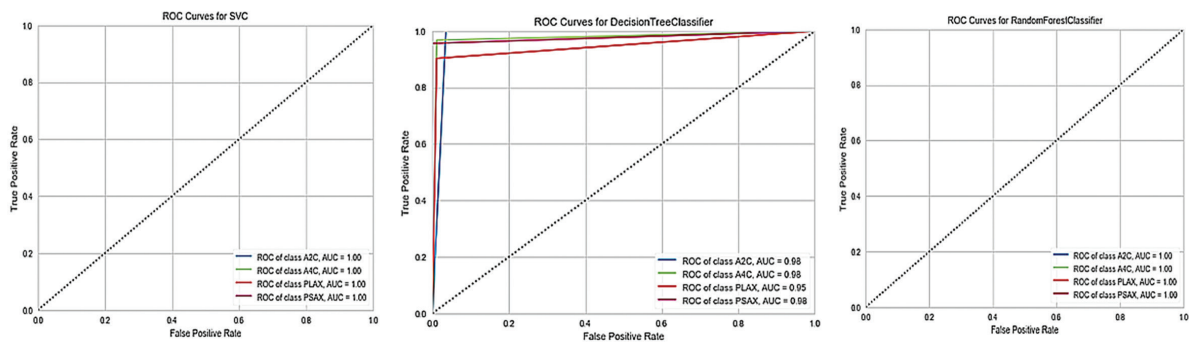


Fig. 8. ROC curve of AKAZE with SVM, Decision Tree and Random Forest classifier

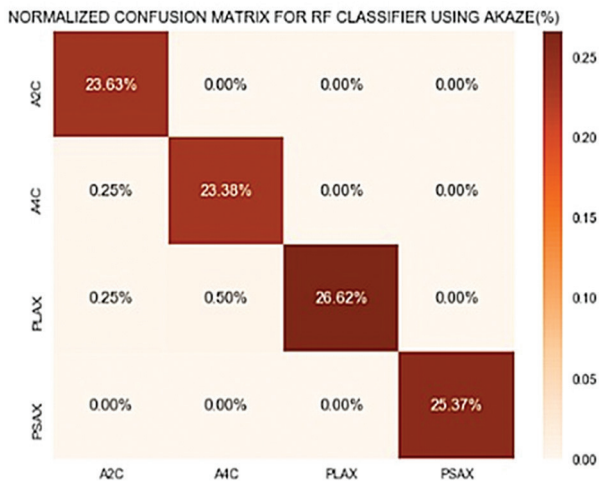


Fig. 9. Confusion matrix of Random Forest classifier using AKAZE

The confusion matrix allows a more in-depth examination of the model's behavior. Here, we only presented the confusion matrix for the model that employed the AKAZE method for feature extraction and a random forest classifier to produce the best results compared to other models. The features of echocardiographic images are incredibly complex. AKAZE employs a more complex descriptor extraction method than ORB. It results in more accurate, robust, and computationally less expensive echocardiographic image classification results.

5. CONCLUSION AND FUTURE WORK

This study combined ORB-AKAZE-based feature extraction with BOVW to classify echocardiogram images into four primary views. Automated view classification will make it easier to complete subsequent cardiac echo tasks, such as disease prediction and segmenting the region of interest. The ensembling technique Random Forest classifier outperformed both SVM and decision tree in predicting the views of echo images. Handcrafted features are typically not robust for large datasets and are computationally intensive. Future research will need to incorporate additional echocardiographic views, such as the apical five-chamber (A5C), apical three-chamber (A3C), and others, into our model. Our current research focuses on automated deep-learning feature extraction for cardiac echocardiographic images.

DATA AVAILABILITY

Due to reasonable privacy and security concerns, the datasets used in this study are not publicly available. The datasets were collected from Aster MIMS Hospital Kottakal, Kerala, India. The authors make de-identified data available upon reasonable request and with permission from the Institutional Ethics Committee (EC/13/2021 dated 25th March 2021). Experiments carried out following applicable laws and regulations. We want to extend thanks to the members of Aster MIMS (doctors, echo technicians, and staff) for their cooperation.

CODE AVAILABILITY:

<https://github.com/shamlabeevia/2D-Echocardiographic-View-classification>

6. REFERENCES:

- [1] D. Ghorbani et al. "Deep learning interpretation of echocardiograms", NPJ Digital Medicine, Vol. 3, No. 1, 2020, pp. 1-10.
- [2] F. Pereira et al. "Automated detection of coarctation of the aorta in neonates from two-dimensional echocardiograms", Journal of Medical Imaging, Vol. 4, No. 1, 2017, pp. 014502-014502.
- [3] H. Moghaddasi, S. Nourian, "Automatic assessment of mitral regurgitation severity based on extensive textural features on 2d echocardiography videos", Computers in Biology and Medicine, Vol. 73, 2016, pp. 47-55.
- [4] A. Madani, R. Arnaout, M. Mofrad, R. Arnaout, "Fast and accurate view classification of echocardiograms using deep learning", NPJ Digital Medicine, Vol. 1, No. 1, 2018, pp. 1-8.
- [5] H. Khamis, G. Zurakhov, V. Azar, A. Raz, Z. Friedman, D. Adam, "Automatic apical view classification of echocardiograms using a discriminative learning dictionary", Medical Image Analysis, Vol. 36, 2017, pp. 15-21.

- [6] H. Vaseli et al. "Designing lightweight deep learning models for echocardiography view classification", *Medical Imaging 2019: Image-Guided Procedures, Robotic Interventions, and Modeling*, Vol. 10951, 2019, pp. 93-99.
- [7] A. A Roest, A. De Roos, "Imaging of patients with congenital heart disease", *Nature Reviews Cardiology*, Vol. 9, No. 2, 2012, pp. 101-115.
- [8] C. A. Duarte-Salazar, A. E. Castro-Ospina, M. A. Becerra, E. D. Trejos, "Speckle noise reduction in ultrasound images for improving the metrological evaluation of biomedical applications: an overview", *IEEE Access*, Vol. 8, 2020, pp.15983-15999.
- [9] F. Benzarti, H. Amiri, "Speckle noise reduction in medical ultrasound images", arXiv:1305.1344, 2013.
- [10] Y. Yu, S. T. Acton, "Speckle reducing anisotropic diffusion", *IEEE Transactions on Image Processing*, Vol. 11, No. 11, 2002, pp. 1260-1270.
- [11] E. Rublee, V. Rabaud, K. Konolige, G. Bradski, "Orb: An efficient alternative to sift or surf", *Proceedings of the International Conference on Computer Vision*, Barcelona, Spain, 6-13 November 2011, pp. 2564-2571.
- [12] P. Chhabra, N. K. Garg, M. Kumar, "Content-based image retrieval system using orb and sift features", *Neural Computing and Applications* Vol. 32, No. 7, 2020, pp. 2725-2733.
- [13] S. B. Kibria, M. S. Hasan, "An analysis of feature extraction and classification algorithms for dangerous object detection", *Proceedings of the 2nd International Conference on Electrical & Electronic Engineering*, Rajshahi, Bangladesh, 27-29 December 2017, pp. 1-4.
- [14] J. Jiang, D. Wu, Z. Jiang, "A correlation-based bag of a visual word for image classification", *Proceedings of the IEEE 3rd Information Technology and Mechatronics Engineering Conference*, Chongqing, China, 3-5 October 2017, pp. 891-894.
- [15] C. D. Căleanu, G. Simion, "A bag of features approach for cause liver lesions investigation", *Proceedings of the 42nd International Conference on Telecommunications and Signal Processing*, Budapest, Hungary, 1-3 July 2019, pp. 323-326.
- [16] D. P. Tian, "A review on image feature extraction and representation techniques", *International Journal of Multimedia and Ubiquitous Engineering*, Vol. 8, No. 4, 2013, pp. 385-396.
- [17] K. A. Jothi, S. Subburam, V. Umadevi, K. Hemavathy, "Heart disease prediction system using machine learning", *Materials Today: Proceedings*, 2021.
- [18] M. A. Alim, S. Habib, Y. Farooq, A. Rafay, "Robust heart disease prediction: a novel approach based on significant feature and ensemble learning model", *2020 3rd International Conference on Computing, Mathematics and Engineering Technologies*, Sukkur, Pakistan, 29-30 January 2020, pp. 1-5.
- [19] S. D. Thepade, K. Jadhav, "Covid-19 identification from chest x-ray images using local binary patterns with assorted machine learning classifiers", *Proceedings of the IEEE Bombay Section Signature Conference*, Mumbai, India, 2020, pp. 46-51.
- [20] A. Naseri, A. Rezaei Nasab, "Automatic identification of minerals in thin sections using image processing", *Journal of Ambient Intelligence and Humanized Computing*, 2021, pp. 1-13.
- [21] Yang, Z., Xu, Q., Bao, S., Cao, X., Huang, Q., "Learning with Multiclass AUC: theory and algorithms", *IEEE Transactions on Pattern Analysis and Machine Intelligence*, 2021, Vol. 44, No. 11, pp. 7747-7763.